

# Solvatochromic Effect on the Photoluminescence of MoS<sub>2</sub> Monolayers

Nannan Mao, Yanfeng Chen, Dameng Liu, Jin Zhang, and Liming Xie\*

Two-dimensional (2D) materials have attracted intense interest because of their unique structure<sup>[1]</sup> and physical properties.<sup>[2]</sup> Much work has been done on 2D transition-metal dichalcogenide monolayers because of their direct bandgaps,<sup>[1b,3]</sup> and potential nanoelectronic and optoelectronic applications.<sup>[1a,2f,4]</sup> For example, MoS<sub>2</sub> and WS<sub>2</sub> monolayers have intense and valley-selective photoluminescence (PL),<sup>[2f,4]</sup> which has potential applications in valleytronics. Transistors fabricated from MoS<sub>2</sub> monolayers showed high performance (>10<sup>8</sup> on/off ratio and moderate carrier mobility up to 200 cm<sup>2</sup> Vs<sup>-1</sup>)<sup>[2d]</sup> and have been integrated into circuits.<sup>[2a,b]</sup> The optical and electrical properties of 2D semiconductors should change with the surrounding environment because of their atomically thin nature. This could be used in bandgap engineering, carrier mobility engineering,<sup>[2d,5]</sup> and sensing.<sup>[6]</sup> The carrier mobility of MoS<sub>2</sub> monolayers can be enhanced by about 100 times with high- $\kappa$  dielectric gating<sup>[2d]</sup> or polymer electrolyte gating.<sup>[5]</sup>

Transition-energy shifts in different surrounding environments, traditionally called solvatochromism, have been widely investigated for fluorophores,<sup>[7]</sup> quantum dots,<sup>[8]</sup> and carbon nanotubes.<sup>[9]</sup> Depending on the molecule/nanomaterial and the surrounding solvent, solvatochromism (usually measured by absorption or fluorescence) can be positive (redshift) or

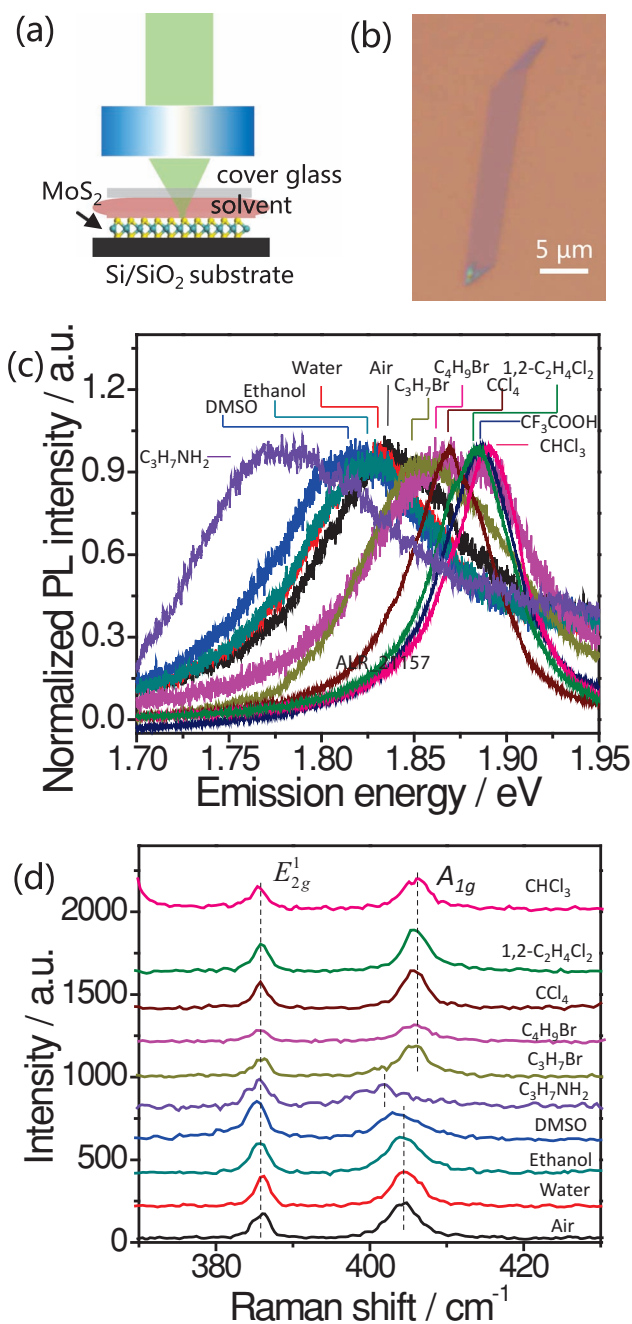


Figure 1. a) Illustration of the experimental configuration. b) Typical optical image of a MoS<sub>2</sub> monolayer. c) PL and d) Raman spectra of MoS<sub>2</sub> monolayers with different solvent surroundings.

N. N. Mao, Dr. Y. F. Chen, Prof. L. M. Xie  
Key Laboratory of Standardization  
and Measurement for Nanotechnology  
of Chinese Academy of Sciences  
National Center for Nanoscience and Technology  
Beijing 100190, PR China  
E-mail: xielm@nanoctr.cn

N. N. Mao, Prof. J. Zhang  
Center for Nanochemistry  
Beijing National Laboratory for Molecular Sciences  
Key Laboratory for the Physics and Chemistry of Nanodevices  
State Key Laboratory for Structural Chemistry  
of Unstable and Stable Species  
College of Chemistry and Molecular Engineering  
Peking University  
Beijing 100871, PR China

Prof. D. M. Liu  
The State Key Laboratory of Tribology  
Department of Precision Instruments and Mechanology  
Tsinghua University  
Beijing 100084, PR China

DOI: 10.1002/sml.201202982



negative (blueshift) with maximum shifts up to hundreds of meV.<sup>[7b]</sup> Many applications have been explored based on solvatochromism, such as probing local polarity in micelles<sup>[10]</sup> and cells.<sup>[11]</sup> Since 2D monolayer semiconductors have a large exciton binding energy,<sup>[12]</sup> the excitonic transition energy should have a large solvatochromic shift. However, solvatochromism of 2D materials has not been reported yet. Herein, we investigate the effect of surrounding solvents on the PL of MoS<sub>2</sub> monolayers. It is revealed that, compared with PL in air, the PL from the MoS<sub>2</sub> monolayer shows redshifts (up to -60 meV) with nonhalogenated solvent surroundings, but blueshifts (up to 60 meV) and a large intensity increase (up to 50 times) with halogenated solvent surroundings.

**Figure 1a** shows the micro-Raman-PL experimental configuration, in which the top side of the MoS<sub>2</sub> monolayer was covered by different solvents during experiments. A typical optical image of the MoS<sub>2</sub> monolayer is shown in **Figure 1b**. MoS<sub>2</sub> monolayers showed a red contrast of about 10%, the  $E_{2g}^1$  Raman mode at 386 cm<sup>-1</sup>, and the  $A_{1g}$  Raman mode at 404 cm<sup>-1</sup>.<sup>[13]</sup> With air surroundings, the MoS<sub>2</sub> monolayer showed a strong emission peak at ≈1.84 eV, corresponding to a direct excitonic transition at the K point.<sup>[1b,3]</sup> PL spectra of MoS<sub>2</sub> monolayers with different solvent surroundings are shown in **Figure 1c**, with an emission peak in the range of 1.78 to 1.90 eV. PL emission from the MoS<sub>2</sub> monolayer was redshifted when the surroundings changed from air to non-halogenated solvents (water, ethanol, dimethyl sulfoxide (DMSO), propylamine), but blueshifted when the surroundings changed from air to halogenated solvents (trifluoroacetic acid, methylene chloride, chloroform, carbon tetrachloride, butyl bromide, propyl bromide). Raman characterization

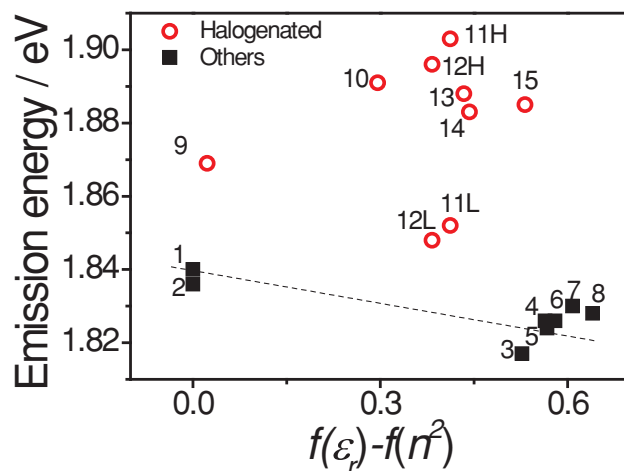


**Figure 2.** Plot of emission energy of the MoS<sub>2</sub> monolayer against  $f(\epsilon_r) - f(n^2)$  of surrounding solvents. The black dashed line is to guide the eye. The numbers near data points are the corresponding solvent numbers assigned in Table 1. The 11H/L and 12H/L represent two emission peaks for solvents 11 and 12, respectively.

showed that the  $A_{1g}$  mode of the MoS<sub>2</sub> monolayer upshifted by ≈1.5 cm<sup>-1</sup> in halogenated solvents and downshifted by ≈4 cm<sup>-1</sup> in propylamine, thus indicating significant p-doping and n-doping of the MoS<sub>2</sub> monolayer,<sup>[14]</sup> respectively. For other solvent surroundings, no obvious Raman shift was observed (**Figure 1d** and **Table 1**), which suggests no doping or straining of the MoS<sub>2</sub> monolayer.

Generally, the emission energy shift  $\Delta E$  in solvatochromism is related to the dielectric constant  $\epsilon_r$  and

**Table 1.** Refractive index, dielectric constant, and  $f(\epsilon_r) - f(n^2)$  of solvents used in the experiments, and MoS<sub>2</sub> monolayer emission energy, emission intensity, and  $A_{1g}$  frequency in different solvent surroundings. Only selected Raman and PL spectra for different solvent surroundings are shown in **Figure 1c** and **d**. The maximum emission intensity of MoS<sub>2</sub> monolayers in different solvents was calibrated by the Si 520 cm<sup>-1</sup> Raman intensity.

Entry	Solvent	$n^a$	$\epsilon_r^a$	$f(\epsilon_r) - f(n^2)$	Emission energy [eV]	Emission intensity [a.u.]	$A_{1g}$ frequency [cm <sup>-1</sup> ]
1	air	1.000	1	0.000	1.840	$2.4 \times 10^2$	404.3
2	hexane	1.375	1.89	0.000	1.836	$2.9 \times 10^2$	404.6
3	dimethyl sulfoxide	1.478	47.2	0.527	1.817	$2.1 \times 10^2$	404.0
4	formamide	1.448	111	0.564	1.826	$2.2 \times 10^2$	404.7
5	acetone	1.362	21.0	0.567	1.824	$2.1 \times 10^2$	404.3
6	ethanol	1.361	25.3	0.580	1.826	$2.4 \times 10^2$	404.3
7	acetonitrile	1.346	36.6	0.608	1.830	$2.1 \times 10^2$	404.5
8	water	1.333	80.1	0.640	1.828	$2.7 \times 10^2$	404.4
9	carbon tetrachloride	1.460	2.24	0.023	1.869	$1.1 \times 10^4$	405.4
10	chloroform	1.446	4.81	0.296	1.891	$1.0 \times 10^4$	405.9
11	propyl bromide	1.434	8.09	0.412	1.903/1.852 <sup>b)</sup>	$3.9 \times 10^2$	405.6
12	butyl bromide	1.440	7.01	0.383	1.896/1.848 <sup>b)</sup>	$4.1 \times 10^2$	405.9
13	methylene chloride	1.424	8.93	0.434	1.888	$1.1 \times 10^3$	405.5
14	1,2-dichloroethane	1.444	10.4	0.443	1.883	$1.0 \times 10^4$	405.7
15	trifluoroacetic acid	1.285	8.55	0.532	1.885	$4.1 \times 10^4$	- <sup>c)</sup>
16	propylamine	1.388	5.31	0.349	1.774	82	400.8

<sup>a)</sup>Data are from Lange's Handbook of Chemistry, 15th edition; <sup>b)</sup>Two emission components were observed and fitted; <sup>c)</sup>The  $A_{1g}$  mode was not observed due to high background.

refractive index  $n$  of the solvent, and further can be expressed by<sup>[7a,9a]</sup>  $\Delta E \propto -(\alpha_e - \alpha_g)[f(\epsilon_r) - f(n^2)]$  where  $\alpha_e$  and  $\alpha_g$  are the polarizabilities of the excited state and the ground state, respectively, and  $f(x) = \frac{2(x-1)}{2x+1}$  is the Onsager polarity function;  $f(\epsilon_r) - f(n^2)$  is responsible for different interaction terms, such as dipole–dipole, dipole–induced dipole, and dispersion interactions.<sup>[7a]</sup> Table 1 shows the MoS<sub>2</sub> monolayer emission energy, emission intensity, and  $A_{1g}$  frequency, together with  $\epsilon_r$  and  $n$  of the surrounding solvents.

**Figure 2** plots the MoS<sub>2</sub> monolayer emission energy in dependence on  $f(\epsilon_r) - f(n^2)$ . Since there is significant doping for halogenated solvents (entries 9–15 in Table 1) and propylamine (entry 16 in Table 1), we first looked into other solvents (entries 1–8 in Table 1). For solvents 1–8, the PL emission redshifts as  $f(\epsilon_r) - f(n^2)$  increases (black squares in Figure 2), which means more stabilization for the excited state in polar solvents. This is similar to the observed redshift of the transition energy for quantum dots<sup>[8]</sup> and carbon nanotubes<sup>[9]</sup> in polar solvents, mainly attributable to the larger dielectric screening in polar solvents.

In contrast to the redshift observed for nonhalogenated solvent surroundings, the PL from MoS<sub>2</sub> monolayers in halogenated solvent surroundings showed blueshifts. Specific bonding of halogen atoms to MoS<sub>2</sub> could affect the emission energy of the MoS<sub>2</sub> monolayer. Reference work has shown that chlorine and bromine can bind to the van der Waals gap between MoS<sub>2</sub><sup>[15]</sup> and WS<sub>2</sub><sup>[16]</sup> layers, respectively, which can give intense PL at low temperature. This is attributed to the bound excitons near neutral halogen atoms. However, bound excitons near halogen atoms should show a redshift,<sup>[15,16]</sup> and cannot explain the blueshift of PL from MoS<sub>2</sub> monolayers in halogenated solvent surroundings.

Several other studies also reported that bound excitons near impurities could introduce an emission peak at the lower-energy side.<sup>[17]</sup> But this is also not the case here because 1) the MoS<sub>2</sub> monolayer samples were cleaved from high-quality single crystals and should have a high quality; 2) emission from bound excitons near impurities can only be observed at low temperatures ( $T < 175$  K)<sup>[17b,c]</sup> and not at room temperature; and 3) emission from bound excitons near impurities is located at  $\approx 1.80$  eV, significantly lower than the observed emission peaks in this work (1.82–1.84 eV in solvents without doping effect and 1.85–1.90 eV for halogenated solvents).

One possibility for the abnormal blueshift observed for halogenated solvent surroundings could be p-doping-induced dissociation of charged excitons (i.e., trions) to neutral excitons. Electrical gating experiments have shown trion formation in MoS<sub>2</sub> and MoSe<sub>2</sub> monolayers.<sup>[18]</sup> Trion emission even dominates the PL spectrum of the as-prepared MoS<sub>2</sub> monolayer due to the intrinsic n-type nature of MoS<sub>2</sub> monolayers.<sup>[18a]</sup> The trion binding energy is  $\approx 20$ –50 meV depending on the carrier concentration.<sup>[18]</sup> By applying a negative gate, electrons can be extracted from the MoS<sub>2</sub> monolayer and then negative trions dissociate to neutral excitons. In PL measurements, the low-energy trion emission disappeared and higher-energy exciton emission was observed.<sup>[18a]</sup> For MoS<sub>2</sub> monolayers in air, the electron density is  $\approx 10^{13}$  cm<sup>-2</sup>,<sup>[2d,14,18a,19]</sup> whereas for MoS<sub>2</sub> monolayers with halogenated solvent surroundings, the carrier (electron) density decreased by  $\approx 4 \times 10^{12}$  cm<sup>-2</sup>

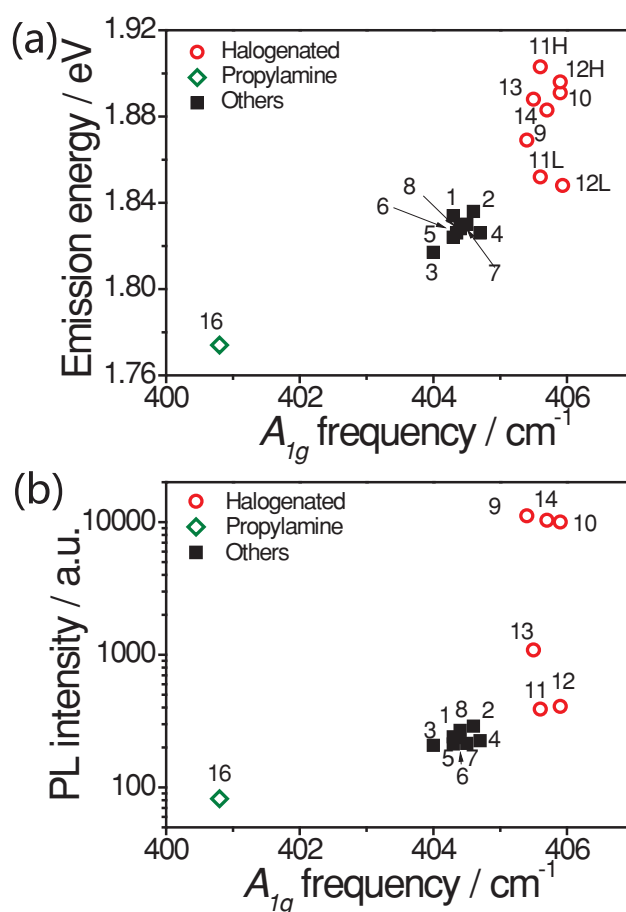


**Figure 3.** Plots of a) emission energy and b) emission intensity against  $A_{1g}$  frequency for MoS<sub>2</sub> monolayers in different solvent surroundings. The numbers near data points are the corresponding solvent numbers assigned in Table 1. The 11H/L and 12H/L represent two emission peaks for solvents 11 and 12, respectively.

according to the  $A_{1g}$  upshift of  $\approx 1.5$  cm<sup>-1</sup>.<sup>[14]</sup> Therefore halogenated solvents extracted electrons from MoS<sub>2</sub>, and then played a similar role to negative electrical gating. As a result, a blueshift was observed for MoS<sub>2</sub> monolayers with halogenated solvent surroundings due to the spectrum weight shift from trion emission to exciton emission.

**Figure 3a** and **b** show emission peak energy and emission intensity against  $A_{1g}$  frequency. The emission energy difference (10–60 meV) between MoS<sub>2</sub> monolayers in halogenated solvents and in air matches well with the trion and exciton energy difference (20–50 meV).<sup>[18a]</sup> Additionally, about 2–50 times stronger PL was observed in halogenated solvents than in air (Figure 3b). This emission intensity increase is consistent with higher PL emission for excitons than that for trions observed in electrical gating experiments.<sup>[18a]</sup> The low emission intensity for trions could be due to faster nonradiative decays.<sup>[20]</sup> Additionally, the emission spectra of MoS<sub>2</sub> monolayers in propyl bromide and butyl bromide show two emission components, which could be due to simultaneous trion and exciton emissions, but this needs further verification. Finally, for propylamine surroundings, the large redshift could be due to increased trion binding energy when the MoS<sub>2</sub> monolayer is more n-doped.<sup>[18a]</sup>

In conclusion, the effect of solvent surroundings on 2D MoS<sub>2</sub> monolayer has been investigated, and shows emission energy tuned from 1.78 to 1.90 eV. The general solvatochromism mechanism still works for solvents without doping effect. For halogenated solvents showing a doping effect, an abnormal blueshift and large PL intensity increase were observed, which were attributed to dissociation of negative trions to neutral excitons. The environment-sensitive PL emission of MoS<sub>2</sub> monolayers could have potential applications in sensing and bioimaging.

## Experimental Section

MoS<sub>2</sub> single crystals were purchased from SPI Supplies. MoS<sub>2</sub> monolayers were mechanically exfoliated on Si/SiO<sub>2</sub> substrates (oxide thickness of 300 nm). Optical images were taken on an Olympus BX51 microscope equipped with a 100× objective and DP71 camera. Micro-Raman-PL measurements were performed on a JY Horiba HR800 system. A long-working-distance 50× objective was used for laser focusing and signal collecting. An 1800 grooves mm<sup>-1</sup> grating was used to disperse the Raman-PL signal, corresponding to a spectral resolution of ≈0.4 cm<sup>-1</sup>. Optical contrast (red contrast of ≈10%) and Raman characterization ( $E_{2g}^{-1}$  at 404 cm<sup>-1</sup> and  $A_{1g}$  at 386 cm<sup>-1</sup>) were used to locate and identify monolayers.<sup>[13]</sup>

All solvents were of analytical purity and purchased from Beijing Tongguang Fine Chemical Company. In micro-Raman-PL measurements, the solvent layer was kept as thin as ≈100 μm to avoid focus distortion. All measurements were performed at room temperature. To avoid laser heating on MoS<sub>2</sub> monolayers in different surroundings, the laser power was kept at ≈0.7 mW, corresponding to a power density of ≈0.7 mW μm<sup>-2</sup>. No Raman or PL shift was observed at or below this laser power.

## Acknowledgements

L.M.X. acknowledges China MOST 2011CB932803. J.Z. acknowledges NSFC (21233001, 21129001).

[1] a) Q. H. Wang, K. Kalantar-Zadeh, A. Kis, J. N. Coleman, M. S. Strano, *Nat. Nanotechnol.* **2012**, *7*, 699–712; b) K. F. Mak, C. Lee, J. Hone, J. Shan, T. F. Heinz, *Phys. Rev. Lett.* **2010**, *105*, 136805; c) K. S. Novoselov, D. Jiang, F. Schedin, T. J. Booth, V. V. Khotkevich, S. V. Morozov, A. K. Geim, *Proc. Natl. Acad. Sci. USA* **2005**, *102*, 10451–10453; d) K. S. Novoselov, A. K. Geim, S. V. Morozov, D. Jiang, Y. Zhang, S. V. Dubonos, I. V. Grigorieva, A. A. Firsov, *Science* **2004**, *306*, 666–669; e) A. Reina, X. T. Jia, J. Ho, D. Nezich, H. B. Son, V. Bulovic, M. S. Dresselhaus, J. Kong, *Nano Lett.* **2009**, *9*, 30–35; f) L. Song, L. J. Ci, H. Lu, P. B. Sorokin, C. H. Jin, J. Ni, A. G. Kvashnin, D. G. Kvashnin, J. Lou, B. I. Yakobson, P. M. Ajayan, *Nano Lett.* **2010**, *10*, 3209–3215; g) L. Ci, L. Song, C. H. Jin, D. Jariwala, D. X. Wu, Y. J. Li, A. Srivastava, Z. F. Wang, K. Storr, L. Balicas, F. Liu, P. M. Ajayan, *Nat. Mater.* **2010**, *9*, 430–435; h) X. S. Li, W. W. Cai, J. H. An, S. Kim, J. Nah, D. X. Yang, R. Piner, A. Velamakanni, I. Jung, E. Tutuc, S. K. Banerjee, L. Colombo, R. S. Ruoff, *Science* **2009**, *324*, 1312–1314.

[2] a) B. Radisavljevic, M. B. Whitwick, A. Kis, *ACS Nano* **2011**, *5*, 9934–9938; b) H. Wang, L. Yu, Y.-H. Lee, Y. Shi, A. Hsu, M. L. Chin, L.-J. Li, M. Dubey, J. Kong, T. Palacios, *Nano Lett.* **2012**, *12*, 4674–4680; c) F. N. Xia, D. B. Farmer, Y. M. Lin, P. Avouris, *Nano Lett.* **2010**, *10*, 715–718; d) B. Radisavljevic, A. Radenovic, J. Brivio, V. Giacometti, A. Kis, *Nat. Nanotechnol.* **2011**, *6*, 147–150; e) F. N. Xia, T. Mueller, Y. M. Lin, A. Valdes-Garcia, P. Avouris, *Nat. Nanotechnol.* **2009**, *4*, 839–843; f) H. L. Zeng, J. F. Dai, W. Yao, D. Xiao, X. D. Cui, *Nat. Nanotechnol.* **2012**, *7*, 490–493; g) Y. M. Lin, A. Valdes-Garcia, S. J. Han, D. B. Farmer, I. Meric, Y. N. Sun, Y. Q. Wu, C. Dimitrakopoulos, A. Grill, P. Avouris, K. A. Jenkins, *Science* **2011**, *332*, 1294–1297; h) D. Teweldebrhan, V. Goyal, A. A. Balandin, *Nano Lett.* **2010**, *10*, 1209–1218; i) P. Goli, J. Khan, D. Wickramaratne, R. K. Lake, A. A. Balandin, *Nano Lett.* **2012**, *12*, 5941–5945; j) J. Khan, C. M. Nolen, D. Teweldebrhan, D. Wickramaratne, R. K. Lake, A. A. Balandin, *Appl. Phys. Lett.* **2012**, *100*, 043109; k) M. Z. Hossain, S. L. Romyantsev, K. M. F. Shahil, D. Teweldebrhan, M. Shur, A. A. Balandin, *ACS Nano* **2011**, *5*, 2657–2663.

[3] A. Splendiani, L. Sun, Y. B. Zhang, T. S. Li, J. Kim, C. Y. Chim, G. Galli, F. Wang, *Nano Lett.* **2010**, *10*, 1271–1275.

[4] T. Cao, G. Wang, W. P. Han, H. Q. Ye, C. R. Zhu, J. R. Shi, Q. Niu, P. H. Tan, E. Wang, B. L. Liu, J. Feng, *Nat. Commun.* **2012**, *3*, 887.

[5] M. W. Lin, L. Z. Liu, Q. Lan, X. B. Tan, K. S. Dhindsa, P. Zeng, V. M. Naik, M. M. C. Cheng, Z. X. Zhou, *J. Phys. D Appl. Phys.* **2012**, *45*, 345102.

[6] a) Q. Y. He, Z. Y. Zeng, Z. Y. Yin, H. Li, S. X. Wu, X. Huang, H. Zhang, *Small* **2012**, *8*, 2994–2999; b) H. Li, Z. Y. Yin, Q. Y. He, H. Li, X. Huang, G. Lu, D. W. H. Fam, A. I. Y. Tok, Q. Zhang, H. Zhang, *Small* **2012**, *8*, 63–67.

[7] a) P. Suppan, *J. Photochem. Photobiol. A* **1990**, *50*, 293–330; b) C. Reichardt, *Chem. Rev.* **1994**, *94*, 2319–2358.

[8] C. A. Leatherdale, M. G. Bawendi, *Phys. Rev. B* **2001**, *63*, 165315.

[9] a) J. H. Choi, M. S. Strano, *Appl. Phys. Lett.* **2007**, *90*, 223114; b) B. A. Larsen, P. Deria, J. M. Holt, I. N. Stanton, M. J. Heben, M. J. Therien, J. L. Blackburn, *J. Am. Chem. Soc.* **2012**, *134*, 12485–12491; c) C. A. Silvera-Batista, R. K. Wang, P. Weinberg, K. J. Ziegler, *Phys. Chem. Chem. Phys.* **2010**, *12*, 6990–6998.

[10] M. C. Rezende, C. Mascayano, L. Briones, C. Aliaga, *Dyes Pigm.* **2011**, *90*, 219–224.

[11] G. Signore, R. Nifosi, L. Albertazzi, B. Storti, R. Bizzarri, *J. Am. Chem. Soc.* **2010**, *132*, 1276–1288.

[12] A. Ramasubramaniam, *Phys. Rev. B* **2012**, *86*, 115409.

[13] C. Lee, H. Yan, L. E. Brus, T. F. Heinz, J. Hone, S. Ryu, *ACS Nano* **2010**, *4*, 2695–2700.

[14] B. Chakraborty, A. Bera, D. V. S. Muthu, S. Bhowmick, U. V. Waghmare, A. K. Sood, *Phys. Rev. B* **2012**, *85*, 161403.

[15] a) D. Dumchenko, C. Gherman, L. Kulyuk, *J. Optoelectron. Adv. Mater.* **2005**, *7*, 775–779; b) L. Kulyuk, L. Charron, E. Fortin, *Phys. Rev. B* **2003**, *68*, 075314.

[16] L. Kulyuk, D. Dumcehno, E. Bucher, K. Friemelt, O. Schenker, L. Charron, E. Fortin, T. Dumouchel, *Phys. Rev. B* **2005**, *72*, 075336.

[17] a) K. F. Mak, K. L. He, J. Shan, T. F. Heinz, *Nat. Nanotechnol.* **2012**, *7*, 494–498; b) G. Sallen, L. Bouet, X. Marie, G. Wang, C. R. Zhu, W. P. Han, Y. Lu, P. H. Tan, T. Amand, B. L. Liu, B. Urbaszek, *Phys. Rev. B* **2012**, *86*, 081301; c) T. Korn, S. Heydrich, M. Hirmer, J. Schmutzler, C. Schuller, *Appl. Phys. Lett.* **2011**, *99*, 102109.

[18] a) K. F. Mak, K. He, C. Lee, G. H. Lee, J. Hone, T. F. Heinz, J. Shan, *Nat. Mater.* **2012**, doi: 10.1038/nmat3505; b) J. S. Ross, S. Wu, H. Yu, N. J. Ghimire, A. M. Jones, G. Aivazian, J. Yan, D. G. Mandrus, D. Xiao, W. Yao, X. Xu, *arXiv:1211.0072 [cond-mat.mes-hall]* **2012**.

[19] K. Kaasbjerg, K. S. Thygesen, K. W. Jacobsen, *Phys. Rev. B* **2012**, *85*, 115317.

[20] a) D. E. Gomez, J. van Embden, P. Mulvaney, M. J. Fernee, H. Rubinsztein-Dunlop, *ACS Nano* **2009**, *3*, 2281–2287; b) P. P. Jha, P. Guyot-Sionnest, *ACS Nano* **2009**, *3*, 1011–1015.

Received: November 30, 2012  
Revised: January 7, 2013  
Published online: February 26, 2013